American Journal of Plant Sciences, 2024, 15, 467-485
https://www.scirp.org/journal/ajps
ISSN Online: 2158-2750
ISSN Print: 2158-2742

Phenotypic Characterization and QTL/Gene Identification for Internode Number and Length Related Traits in Maize

Jing Li[1*], Fengjuan Gu[1,2*], Guoqiang Wang[1], Yingyi Zhang[1], Xiangling Gong[1], Wei Wei[1], Xianchuang Zhang[1,3], Lin Liu[1,4], Hameed Gul[1], Hong Duan[1], Chaoxian Liu[1], Qianlin Xiao[1], Zhizhai Liu[1]

[1]College of Agronomy and Biotechnology/Maize Research Institute, Southwest University, Chongqing, China
[2]Health Commission of Suixi County, Huaibei, China
[3]Agriculture and Rural Bureau of Qinglong County, Qinglong County, China
[4]Yunyang Committee of Agriculture and Rural Affairs, Chongqing, China
Email: xiaoql1853@swu.edu.cn, liu003@swu.edu.cn

How to cite this paper: Li, J., Gu, F.J., Wang, G.Q., Zhang, Y.Y., Gong, X.L., Wei, W., Zhang, X.C., Liu, L., Gul, H., Duan, H., Liu, C.X., Xiao, Q.L. and Liu, Z.Z. (2024) Phenotypic Characterization and QTL/Gene Identification for Internode Number and Length Related Traits in Maize. *American Journal of Plant Sciences*, **15**, 467-485.
https://doi.org/10.4236/ajps.2024.157033

Received: April 12, 2024
Accepted: July 20, 2024
Published: July 23, 2024

Abstract

Internode number and length are the foundation to constitute plant height, ear height and the above-ground spatial structure of maize plant. In this study, segregating populations were constructed between EHel with extremely low ear height and B73. Through the SNP-based genotyping and phenotypic characterization, 13 QTL distributed on the chromosomes (Chrs) of Chr1, Chr2, Chr5-Chr8 were detected for four traits of internode no. above ear (INa), average internode length above ear (ILaa), internode no. below ear (INb), and average internode length below ear (ILab). Phenotypic variation explained (PVE) by a single QTL ranged from 6.82% (*qILab*2-2) to 12.99% (*qILaa*5). *Zm00001d016823* within the physical region of *qILaa*5, the major QTL for ILaa with the largest PVE was determined as the candidate through the genomic annotation and sequence alignment between EHel and B73. Product of *Zm00001d016823* was annotated as a WEB family protein homogenous to At1g75720. qRT-PCR assay showed that *Zm00001d016823* highly expressed within the tissue of internode, exhibiting statistically higher expression levels among internodes of IN4 to IN7 in EHel than those in B73 ($P < 0.01$), implying a negative regulating trend to internode elongation in maize. Functional dissection of *Zm00001d016823* might provide novel insight into molecular mechanism beyond phytohormones controlling internode development in maize.

*These authors contributed equally to this work.

Keywords

Maize (*Zea mays* L.), Internode No., Average Internode Length, Phenotypic Characterization, Candidate Gene Discovery

1. Introduction

Plant architecture plays a crucial role in determining the yield performance of maize varieties. Key factors influencing plant architecture are plant height (PH) and ear height (EH). Both PH and EH are closely related to the final yield performance of maize varieties [1] [2]. Therefore, optimizing these factors is crucial for improving the overall productivity of maize. Extensive research has been conducted on PH and EH, resulting in the identification and collection of over 250 quantitative trait loci (QTL) distributed throughout the maize genome (MaizeGDB, http://www.maizegdb.org). Additionally, stalk lodging performance is closely linked to both PH and EH, particularly the ratio of EH to PH (EH/PH). Stalk lodging can have a significant impact on plant architecture and can result in substantial yield losses during maize production [3] [4].

The performances of both PH and EH are determined by the internode no. and length of maize stalk, and significant progress has been made in identifying candidate genes associated with PH, EH, and even internode no. and length related traits in maize [5] [6]. Phytohormones play important roles in structuring many tissues in plants [7]-[9]. And genes involved in biosynthesis, signaling, and regulating of phytohormones, including auxin, CK, GA, and BR, are intensively documented in maize for their significant potential roles in stress responding and organ growth and development [10]-[13]. Dwarf plant related genes, such as *dwarf plant1* (*d1*)/*3*/*8*/*9* that are involved in GA biosynthesis or signal transduction, are reported to control both PH and EH in maize [14]-[17]. A recent report documented by Paciorek and colleagues of Bayer Crop Science demonstrated that the suppression of two GA biosynthesis related genes, i.e., *ZmGA20ox3* and *ZmGA20ox5*, resulted in the reduced GA levels in internodes, which finally led to significantly reduced PH and EH in maize [6]. Similar performances of shortened internode lengths and PH caused by the repression of *RIN1* (*REDUCED INTERNODE1*) to two gibberellin-oxidase genes of *GA2ox7a*/*7b* in soybean were also reported and functionally dissected [18]. Another study based on mutant of *m*30 with decreased internode no. and length, documented *ZmCYP90D1* as a candidate gene that was involved in regulating internode development through modulation of BR-mediated cell division and growth [19]. Furthermore, a most recent report documented a novel module of ZmBZR1-ZmIBH1-ZmXTH1 that joint both BR and JA in regulating the internode elongation in maize [20].

Continuous and further gene discovery and functional dissection of height related traits, especially those focused on internodes, could provide informative

references for the understanding of growth and development of internodes, then the regulating of height related traits, and even stalk improvement in maize. Intensively genotyping and omics strategies provide high-throughput and global tools to dissect genes or pathways for candidate traits, such PH, EH, and internode related traits, through whole development stages. Based on B73, Le *et al*. correspondingly collected 12 and 17 mass samples of internodes at elongation (V14) and maturity (R6) stages, and dissected the dynamic transcriptome features and spatiotemporal expression patterns of genes involved in maize internodes via RNA-seq [21]. They discovered vast genes and several regulatory networks for cell elongation and cell division responding to internode development in maize [21]. Another study by Wu and colleagues identified 85 significant SNPs and five candidate genes that were associated with internode length, diameter, and other stalk lodging resistance-related traits. These candidate genes are involved in various biological processes, such as cell division, growth, and hormone signaling pathways [22]. An integrated study of metabolites detection and RAN-seq focused on stalk strength identified >2000 up-regulated genes potentially associated with stalk-lodging resistance in maize, among which 28 genes that encoding cellulose synthase, chitinase, and COBRA-like protein 4 were found to be associated with stalk strength, providing insights into the molecular mechanisms underlying this trait [23].

In the previous work of germplasm characterization and improvement, a distinct inbred line of EHel with extremely low EH was identified [24]. The ratio of EH/PH of EHel is less than 0.25, extremely lower than that of the reference line B73. The corresponding F2 and F2:3 populations were constructed through the crossing of EHel and B73. In the present study, both parental lines of EHel and B73, and F2 were genotyped with chipset-based SNPs. Combining with phenotyping of PH, EH, EH/PH, and internode related traits, we performed candidate gene discovery controlling internode no. and length related traits in maize. The results will deepen and extend our understanding to the growth and development of maize internodes, as well as provide informative references for the construction of idea plant architecture in maize.

2. Materials and Methods

2.1. Plant Materials

Female line of EHel was screened out from the self-pollinating descendants between the cross of Dan 299 and Pioneer hybrids ten years ago [24]. The typical character of EHel is the extremely low ratio of EH/PH, less than 30% to that of B73. In the spring of 2016, we collected pollens from B73, and crossed with EHel. The F1 seeds were planted and all F1 plants were self-pollinated to construct F2 in 2017. In the next spring, one F2 ear was randomly selected and planted, and F2:3 family lines were constructed with the self-pollinating of F2 individuals. In the present study, both parental lines of EHel and B73, and populations of F2 and F2:3 were used for the phenotyping, genotyping, QTL map-

ping, and further candidate gene discovering.

2.2. Phenotyping and Data Analyzing

In the spring of 2019, EHel, B73, and 127 family lines of F2:3 were all planted in the field of college farm in Xiema(29˚45'39" N, 106˚ 23'32" E, Beibei, Chongqing, China) with the same experimental design described by Gul *et al*. [24]. One week after anthesis, 10 continuous plants of each F2:3 family line were labelled, and the phenotypic datasets of PH and EH were collected referred to Shi *et al*. and Norman *et al*. [25] [26]. At harvesting time, all leaves and leaf sheaths of these same 10 plants of each family line were removed, and datasets of four internode related traits, including internode number above ear (INa), internode length above ear (ILa), internode number below ear (INb), and internode length below ear (ILb) were collected. Then the average internode length above ear (ILaa) and average internode length below ear (ILab) were calculated accordingly. When collecting the datasets of these four traits, the node that bearing the topmost ear was labelled as the initiation internode, and the internodes above the topmost ear were correspondingly marked as IN1, IN2, IN3, etc. in ascending order based on the distance between internodes and the labelled node. On the contrary, all internodes below the topmost ear were marked as IN-1, IN-2, IN-3, etc. in the same way.

All collected datasets were input into Microsoft-Excel 365 to calculate the average and standard deviation (S.D.) and carried out the T-test. SAS (Version 9.0) was used to carry out summary statistics analysis and normal distribution test for the frequency of all traits, as well as the correlation analysis.

2.3. DNA Extraction, Genotyping, and Linkage Map Construction

In the spring of 2018, tips of the 3rd developed leaves of EHel, B73 and 127 individuals of F2 were cut for DNA extraction with CTAB procedure. The extracted DNA solutions with RNase were sent to China Golden Marker Biotechnology Co., Ltd. (Beijing, China) for chipset-based genotyping, as described by Gul *et al*. [24]. Among ~10000 SNPs integrated within the chipset, a total of 2108 polymorphism SNPs between EHel and B73 were screened out for the construction of linkage map via QTL IciMapping V4.5.3 [27].

2.4. QTL Mapping and Genomic Annotation of Target QTL

To detect the QTL for INa, INb, ILaa, and ILab, the ICIM-ADD model implemented in the BIP procedure of QTL IciMapping was used with the procedure of fixed LOD of 2.5 [27]. All detected QTL were named by the way described by McCouch *et al*. [28], while gene action and phenotypic variation explained (PVE, %) of each detected QTL were determined according to Stuber *et al*. [29]. Physical chromosomal region of target QTL was determined according to the integrated information of maize genome database (MaizeGDB, https://www.maizegdb.org/). Candidate genes within the physical region of tar-

get QTL were annotated and described referred to the genomic information of B73 (Maize B73 RefGen_v4).

2.5. Candidate Gene Screening

Referred to Walley *et al.*, RNA-seq based FPKMs among 23 tissues, i.e. tissue 1 to 23, of all annotated genes were collected from MaizeGDB (https://www.maizegdb.org/) [30]. The FPKMs of all annotated genes in the tissue of 7-8 internode (Tissue 2) were standardized to 1, then all the FPKMs of other tissues were divided by that of Tissue 2 for each annotated gene, to get the relative FPKMs of all genes among 23 tissues. According to the annotated description and the relative FPKMs of all genes, *Zm00001d016823* was screened out as the candidate of *qILaa5* with the largest PVE. Another gene, *Zm00001d016831* also exhibited relatively higher FPKMs within the internode tissues (Tissue 1 and 2), and was also screened for sequence comparison.

2.6. Gene Cloning and qRT-PCR Based Validation

Primers of both *Zm00001d016823* (Forward: 5'-ACGATGTCTACTTCACCGCC-3', Reverse: 5'-ATACGGAGCAGCATCTCAGC-3') and *Zm00001d016831* (Forward: 5'-ATATGAAGGTACGCTTGGACCC-3', Reverse: 5'-CCTGTCCTGGTTAGTGAATCCT-3') were designed by the on-line tool of NCBI—Primer BLAST (https://www.ncbi.nlm.nih.gov/tools/primer-blast/) to clone the corresponding sequences from EHel and B73. The PCR products of *Zm00001d016823* and *Zm00001d016831* from EHel and B73, i.e., $Zm00001d016823^{EHel}$, $Zm00001d016823^{B73}$, $Zm00001d016831^{EHel}$, $Zm00001d016831^{B73}$, were sequenced and aligned through DNAMAN (v8.0). Vector NTI advance® v11.5 was used to predict the coding amino acids (aa), and compare the aa sequences between EHel and B73.

During the spring season of 2019, tissues of leaf samples at the middle part of the 8th leaf, immature female inflorescences (about 2 to 3 cm), internodes and leaf sheaths above ground, and roots samples of both EHel and B73 were collected at V12 stage. RNA of all samples were extracted with the kit of DP432 (TianGen Biotech (Beijing) Co., Ltd., Beijing, China). Cause no polymorphisms were detected between $Zm00001d016831^{EHel}$ and $Zm00001d016831^{B73}$, qRT-PCR assays were only focused on *Zm00001d016823* between tissues of EHel and B73 referred to Xiao *et al.* [31]. *actin1* was used as the internal control, and the relative transcription levels were calculated through the method of $2^{-\Delta\Delta CT}$ [32].

3. Results

3.1. Phenotypic Features of Parental Lines and Segregating Populations

The phenotyping results showed that the plant height (PH), ear height (EH), and

ratio of EH/PH of EHel were extremely lower than those of B73 (**Figure 1(A)-(E)**). The phenotypic performances of ILaa, INb, and ILab of EHel were also extremely lower than those of B73 (**Figure 1(F)**; **Figure 1(G)** & **Figure 1(I)**), while the INa exhibited contrary trends in both 2018 and 2019 (**Figure 1(H)**). In addition, except IN5 in 2018, the lengths of all internodes of EHel were statistically lower than those of B73 (**Figure 1(J)** & **Figure 1(K)**).

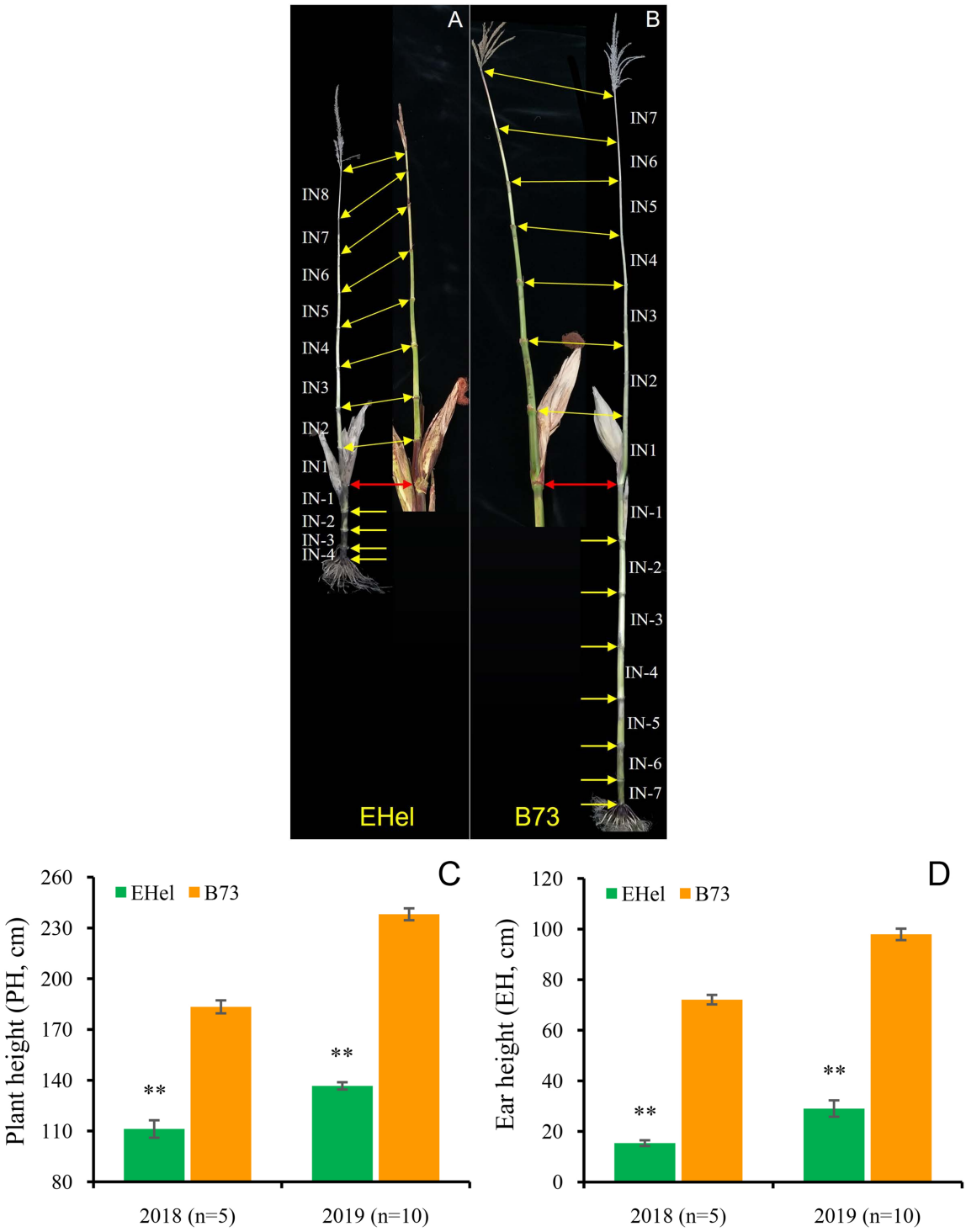

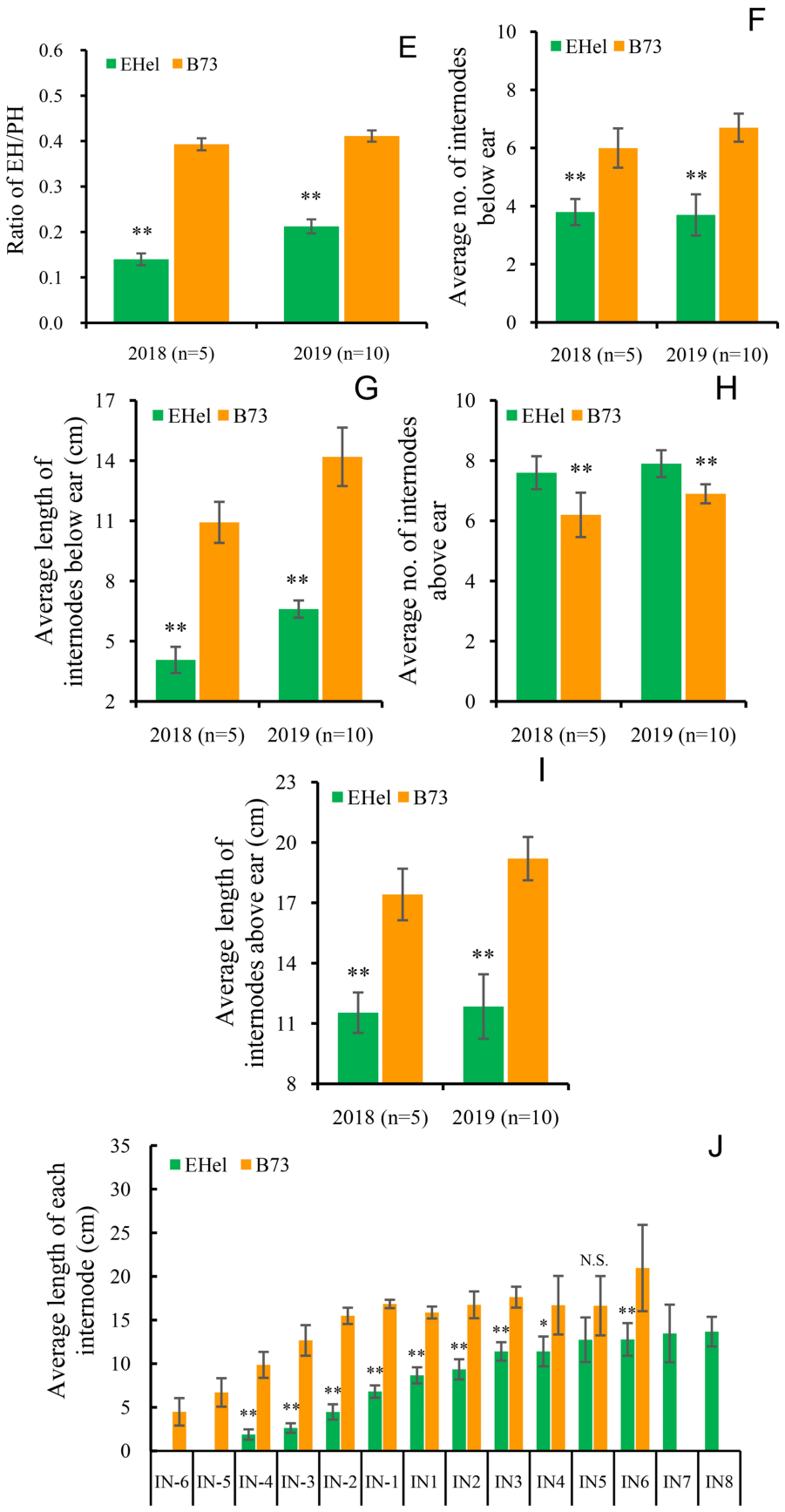
E
Ratio of EH/PH
EHel
B73
2018 (n=5)
2019 (n=10)
F
Average no. of internodes below ear
G
Average length of internodes below ear (cm)
H
Average no. of internodes above ear
I
Average length of internodes above ear (cm)
J
Average length of each internode (cm)
N.S.
IN-6
IN-5
IN-4
IN-3
IN-2
IN-1
IN1
IN2
IN3
IN4
IN5
IN6
IN7
IN8

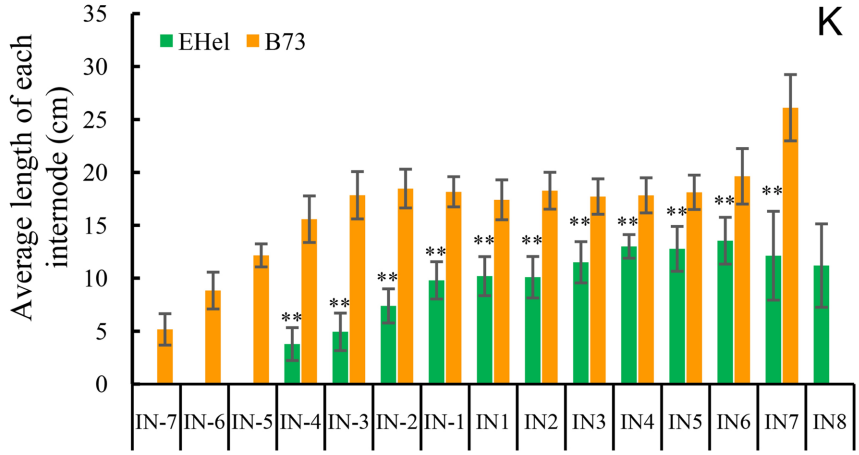

A and B: Internodes of EHel (A) and B73 (B); C to E: Comparisons of plant height (PH, C), ear height (EH, D), and ratio of EH/PH (E) between EHel and B73; F to I: Comparisons of average internode no. (F) and length (G) below ear, and average internode no. (H) and length (I) above ear between EHel and B73; J and K: Comparisons of each internode length between EHel and B73 in 2018 (J, n = 5) and 2019 (K, n = 10). * and ** refer to the corresponding significance levels of $P < 0.05$ and $P < 0.01$, N.S. to no significance. Red arrows refer to the node position of bearing the topmost ear, while yellow arrows to the corresponding nodes above and below the topmost ears of both EHel and B73.

Figure 1. Stalk related phenotypic characterization of EHel and B73.

Correlation analysis among F2:3 family linesshowed that INa presented negative correlations to the other six traits, especially to EH, EH/PH, and ILaa ($P < 0.01$, Table 1). Positive correlations were observed among the trait pairs of PH, EH, EH/PH, INb, ILaa, and ILab, and the P values of all correlation coefficients were less than 0.01 except those of ILab vs EH/PH and ILaa vs INb (Table 1). Specially, we constructed the correlation network among four internode related traits of INa, INb, ILaa, and ILab (Figure 2).Significant correlations were observed among three trait-pairs of INa vs ILaa, ILaa vs ILab, and ILab vs INb, among which INa vs ILaa exhibited significant negative correlation, while positive correlations were detected for the other two pairs (Figure 2).

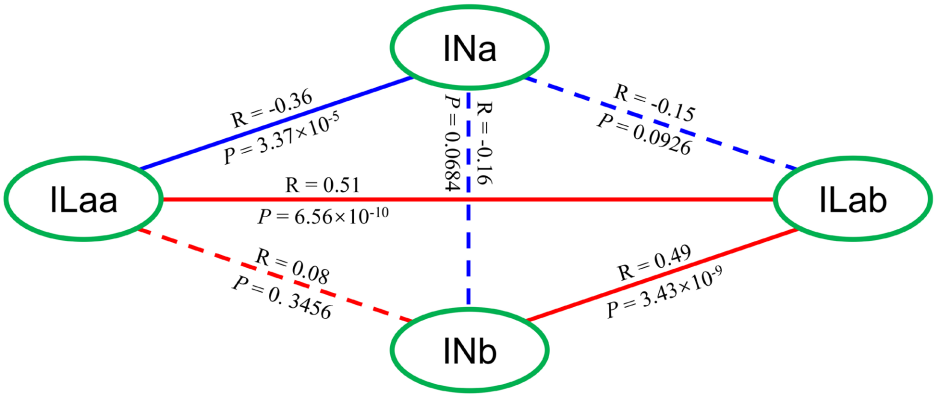

Note: Blue (negative) and red (positive) solid lines refer to significant correlations between the connected traits, while those of blue (negative) and red (positive)dashed lines for non-significant correlations between the connected traits.

Figure 2. Correlation network among four internode related traits.

Table 1. Correlation of seven target traits among F2:3 family lines.

Trait	EH	EH/PH	INa	INb	ILaa	ILab
PH	0.79**	0.58**	−0.05	0.59**	0.57**	0.80**
EH		0.95**	−0.23**	0.82**	0.25**	0.78**
EH/PH			−0.27**	0.81**	0.08	0.67**
INa				−0.16	−0.36**	−0.15
INb					0.08	0.49**
ILaa						0.51**

Note: ** refers to the corresponding significance level of $P < 0.01$.

3.2 Construction of Linkage Map and QTL Mapping

A total of 2108 polymorphic SNPs were screened out between EHel and B73, and the linkage map was constructed through the genotyping of these 2108 SNPs, with a total length of 3299.18 cM and average SNP interval of 1.57 cM (**Figure 3**). Integrated the constructed linkage map and phenotypic performances of INa, INb, ILaa, and ILab of F2:3, 13 QTL were detected for these four traits, including four (*qINa*2, *qINa*7-1, *qINa*7-2, and *qINa*8) for INa, three (*qILaa*1, *qILaa*2, and *qILaa*5) for ILaa, one (*qINb*8) for INb, and five (*qILab*2-1/2/3/4 and *qILab*6) for ILab (**Table 2**). Among these 13 QTL, *qILaa*5 presented the largest PVE (phenotypic variation explained) of 12.99%, followed by *qINa*7-1 (12.19%) and *qINb*8 (12.22%), while the rest 10 possessed PVE less than 10% (**Table 2**).

Table 2. QTL mapping results of four internode related traits.

Trait	QTL	Position (cM)	LOD	PVE (%) [a]	A[b]	D[c]	Gene action	Confidence interval (cM)
INa	*qINa*2	297	2.51	9.89	−0.02	−0.30	OD	292.5 - 299.0
	*qINa*7-1	5	3.06	12.19	−0.26	−0.02	A	3.5 - 7.5
	*qINa*7-2	64	2.69	9.82	0.17	0.28	OD	55.5 - 65.5
	*qINa*8	317	2.72	9.52	−0.10	−0.26	OD	312.5 - 320.5
ILaa	*qILaa*1	300	2.99	8.71	0.61	−0.15	PD	299.5 - 300.5
	*qILaa*2	1	2.94	8.96	−0.45	−0.86	OD	0 - 7.5
	*qILaa*5	303	4.50	12.99	−0.59	0.48	PD	302.5 - 304.5
INb	*qINb*8	338	3.20	12.22	−0.23	0.52	OD	335.5 - 343.5
ILab	*qILab*2-1	3	3.05	7.32	−0.98	0.24	PD	0 -7.5
	*qILab*2-2	176	4.02	6.82	−0.49	0.85	OD	172.5 - 177.5
	*qILab*2-3	200	4.23	6.98	−0.67	0.73	D	197.5 - 203.5
	*qILab*2-4	214	4.16	6.85	−0.72	0.72	D	211.5 - 214.5
	*qILab*6	45	3.77	6.87	−0.61	0.42	PD	44.5 - 47.5

Note: a refers to the phenotypic variation explained, b to additive effect, and c to dominant effect. A, D, PD, and OD of Gene action refer to additive effect, dominant effect, partial dominant effect, and over dominant effect, respectively.

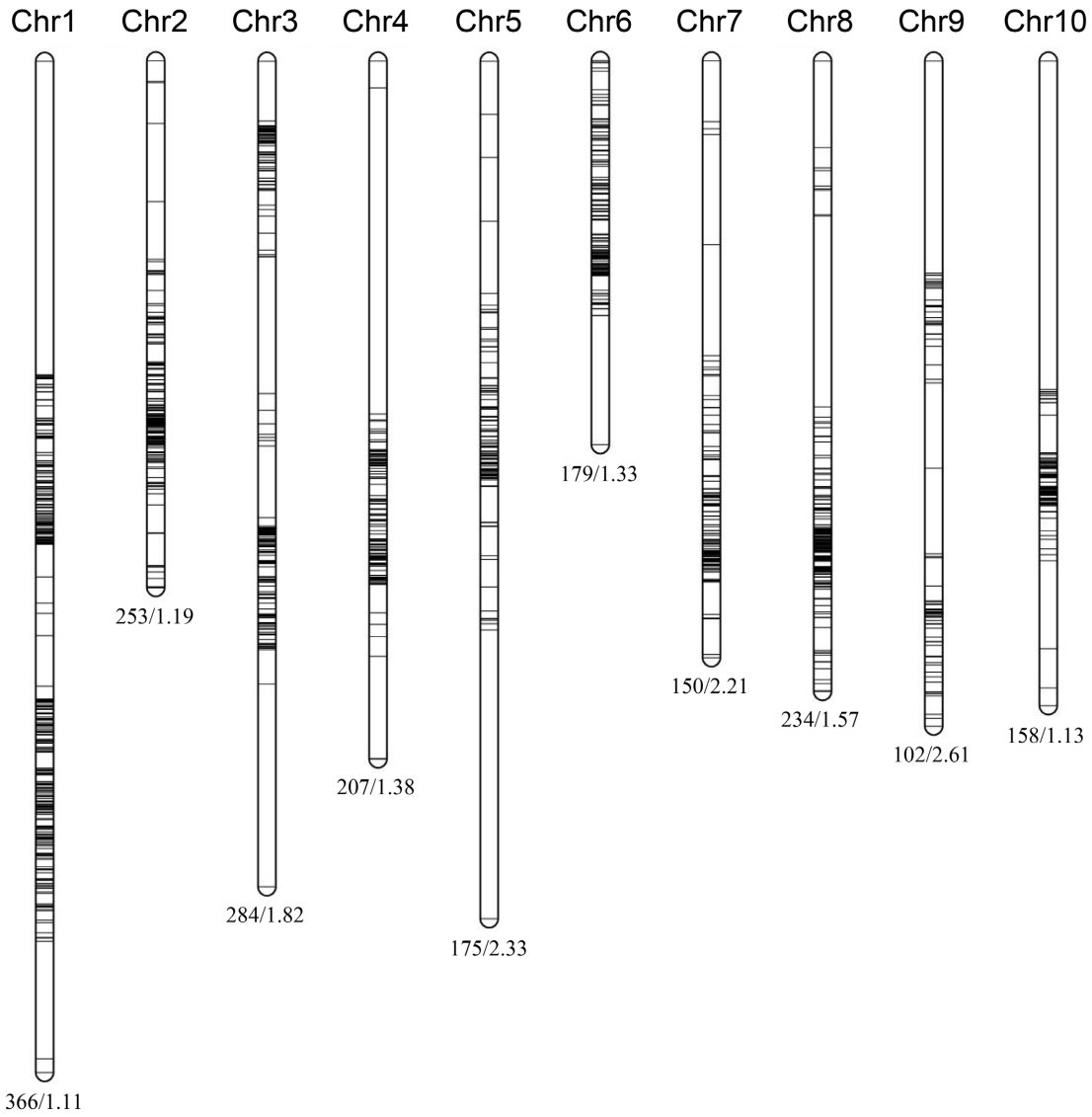

Note: At the bottom of each linkage group (Chr), the figures at the left and right side of "/" refer to the number of SNPs and the average distance (cM) of two adjacent SNPs, respectively.

Figure 3. Construction of linkage map.

3.3. Candidate Gene Discovering for qILaa5

Among all identified QTL, *qILaa*5 presented as the major QTL with the largest PVE for average internode length above ear (ILaa), and candidate genes were discovered for this QTL. Within the physical interval of 1 Mb fixed by the flanking SNPs of *qILaa*5 (177.26 Mb - 178.26 Mb), a total of 28 genes were annotated according to the reference genome of B73 (**Table 3**). Among the annotated genes, 17 genes exhibited expression signals in the tissues of internodes based on the RNA-seq datasets, while only *Zm00001d016823* exhibited the highest relative FPKMs in the tissues of 6 - 7 Internode and 7 - 8 Internode (**Figure 4**). Considering the significant tissue-specific expression patterns, *Zm00001d016823*was screened out as the candidate of *qILaa*5 for further validation.

Table 3. Annotated genes within the physical interval of *qILaa5*.

ID	Gene	Beginning site (bp)	Ending site (bp)	Description
1	*Zm*00001*d*016821	177246416	177261273	Function unknown Hypothetical protein ZEAMMB73_Zm00001d016821 [*Zea mays*]
2	*Zm*00001*d*016822	177260095	177285934	Signal transduction Uncharacterized protein LOC100501806 isoform X1 [*Zea mays*]
3	*Zm00001d016823*	177286413	177287057	Function unknown WEB family protein At1g75720 [*Zea mays*]
4	*Zm*00001*d*016824	177354271	177357801	Recombination and repair uncharacterized protein LOC100280406 [*Zea mays*]
5	*Zm*00001*d*016825	177530082	177539300	Function unknown SPla/RYanodine receptor (SPRY) domain-containing protein [*Zea mays*]
6	*Zm*00001*d*016826	177539021	177540697	Function unknown uncharacterized protein LOC107305671 [*Zea mays*]
7	*Zm*00001*d*016827	177540939	177547554	Chromatin structure and dynamics, Transcription DDT domain-containing protein [*Zea mays*]
8	*Zm*00001*d*016828	177557935	177560415	Function unknown Pentatricopeptide repeat-containing protein At2g27610 [*Zea mays*]
9	*Zm*00001*d*016829	177645936	177646448	No annotation
10	*Zm*00001*d*016830	177739663	177740094	No annotation
11	*Zm00001d016831*	177772939	177774278	Posttranslational modification, protein turnover, chaperones Tubulin-folding cofactor C [*Zea mays*]
12	*Zm*00001*d*016832	177779774	177784519	Function unknown Protein AIG1 [*Zea mays*]
13	*Zm*00001*d*016833	177789995	177803672	No annotation
14	*Zm*00001*d*016834	177813977	177815819	Function unknown uncharacterized LOC100277072 [Zea mays]
15	*Zm*00001*d*016835	177815935	177822681	Translation, ribosomal structure and biogenesis Ligatin [*Zea mays*]
16	*Zm*00001*d*016836	177823355	177829656	Function unknown Rough endosperm3 [*Zea mays*]
17	*Zm*00001*d*016837	177876404	177879393	Posttranslational modification, protein turnover, chaperones Uncharacterized protein LOC100192737 [*Zea mays*]
18	*Zm*00001*d*016838	177880117	177886035	Transcription Auxin response factor 1 [*Zea mays*]
19	*Zm*00001*d*016839	178069833	178070708	Replication, recombination and repair DNA repair protein XRCC3 homolog [*Zea mays*]
20	*Zm*00001*d*016840	178096482	178097375	Posttranslational modification, protein turnover, chaperones E3 ubiquitin-protein ligase EL5 [*Zea mays*]
21	*Zm*00001*d*016841	178195938	178198322	Function unknown Uncharacterized protein LOC100217292 [*Zea mays*]
22	*Zm*00001*d*016842	178210000	178212184	Energy production and conversion, Coenzyme transport and metabolism monooxygenase 1 [*Zea mays*]
23	*Zm*00001*d*016843	178228409	178231973	No annotation

Continued

24	*Zm*00001*d*016844	178232995	178234870	Energy production and conversion, Coenzyme transport and metabolism monooxygenase 1 isoform X3 [*Zea mays*]
25	*Zm*00001*d*016845	178236950	178238261	Function unknown uncharacterized protein LOC100383795 isoform X1 [*Zea mays*]
26	*Zm*00001*d*016846	178239867	178249905	Signal transduction mechanisms probable serine/threonine-protein kinase At1g54610 [*Zea mays*]
27	*Zm*00001*d*016847	178250069	178252558	hypothetical protein ZEAMMB73_Zm00001d016847 [*Zea mays*]
28	*Zm*00001*d*016848	178257482	178258778	Ethylene-responsive transcription factor ERF021 [*Zea mays*]

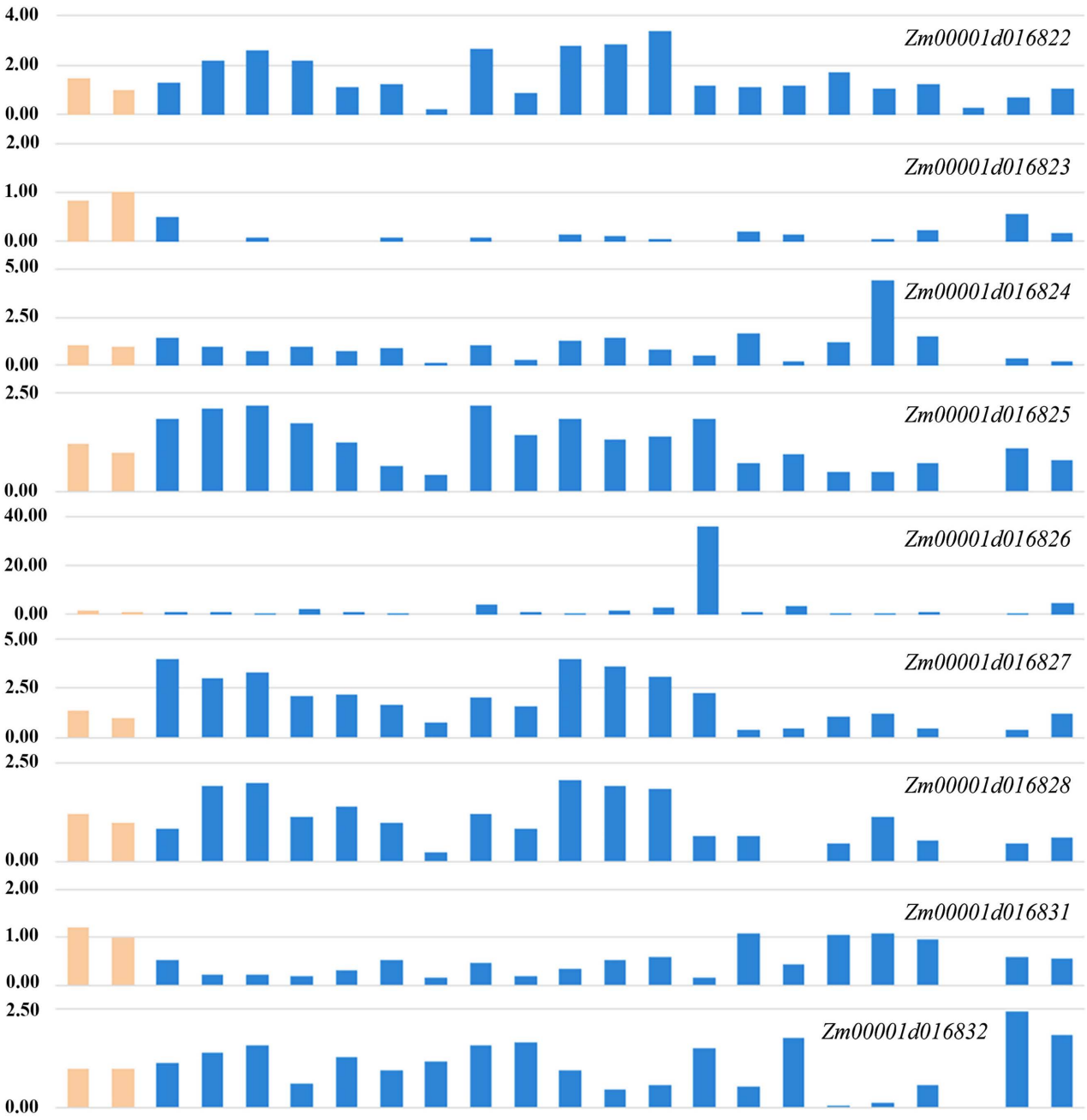

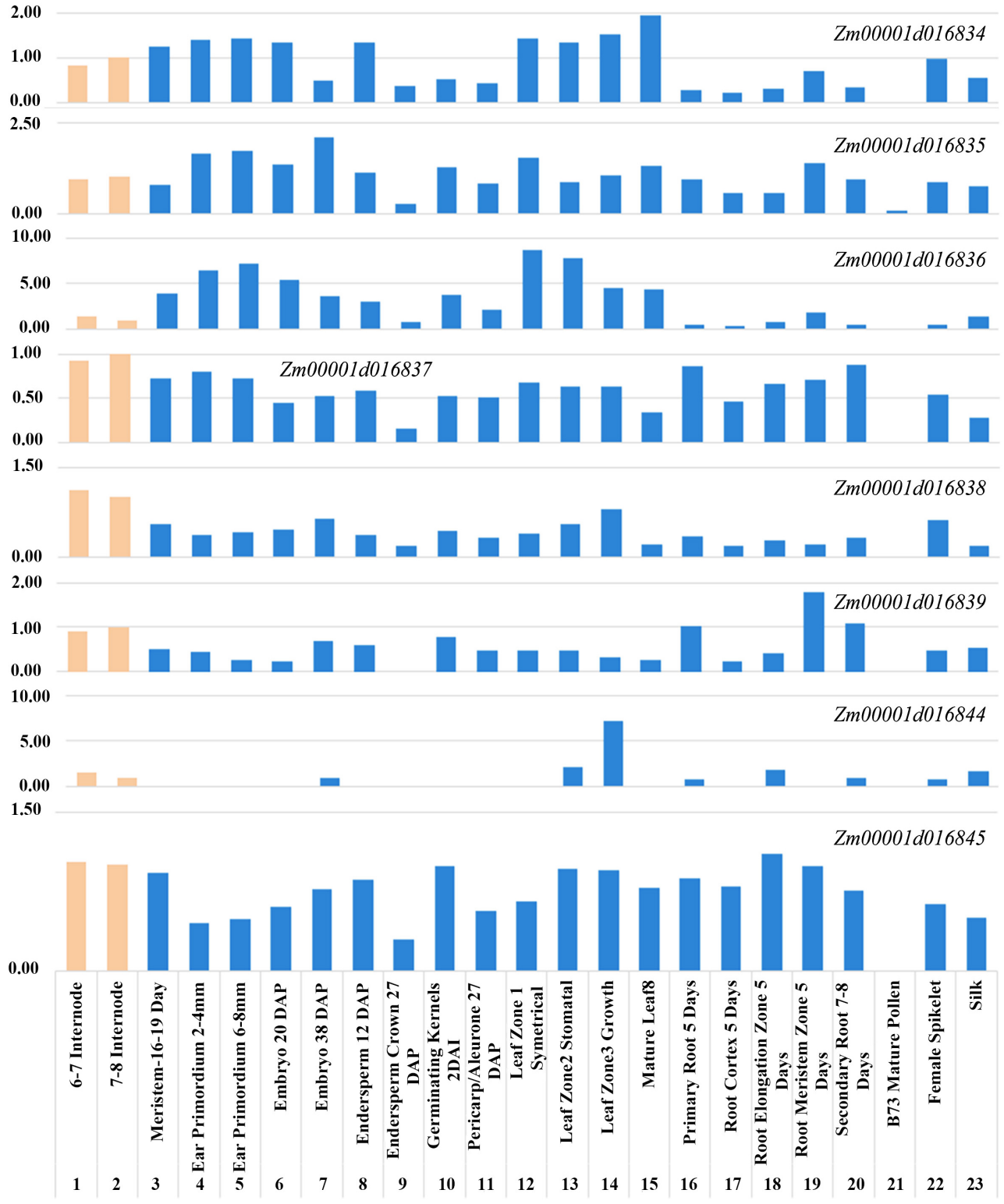

Note: Vertical axis of each section refers to the relative FPKM value of each gene. FKPM values of all genes were referred to Walley *et al.* (2016), and downloaded from MaizeDGB (http://www.maizegdb.org). For each annotated gene, the relative FPKM in the tissue of 7 - 8 Internode (with tissue ID of 2) was standardized to 1, and then the relative expression values of the rest 22 tissues were calculated according to the downloaded FPKMs of the corresponding tissue divided by that of 7 - 8 Internode.

Figure 4. Relative expression patterns of 17 annotated genes among different tissues via RNA-seq.

3.4. Sequence Comparison and qRT-PCR Based Validation

The results of sequence analysis showed that *Zm00001d016823* has only one exon with the coding sequence of 645 bp for 214 amino acids (aa). The sequence of *Zm00001d016823*^{EHel} exhibited 11 polymorphisms to that of *Zm00001d016823*^{B73}, including InDel I (deletion of 12 bp), InDel II (deletion of 6 bp), and 9 SNPs (Figure 5(A)). We also cloned another annotated gene of *Zm00001d016831* that exhibited relatively higher expression levels within the tissues of internodes, while no polymorphisms were detected between the sequences of *Zm00001d016831*^{EHel} and *Zm00001d016831*^{B73} (Figure 5(B)). We compared the coding products by both *Zm00001d016823*^{EHel} and *Zm00001d016823*^{B73}. The results showed that InDel I and II of *Zm00001d016823*^{EHel} led the missing of 6 aa, comparing to the coding product of *Zm00001d016823*^{B73} (Figure 5(C)). Additionally, only the 1st (G in B73 while A in EHel) and 9th (A in B73 while G in EHel) SNPs presented as synonymous mutations, the other 7 SNPs observed within the sequence of *Zm00001d016823*^{EHel} served as nonsynonymous mutations, and led to the changes of aa (Figure 5(C)).

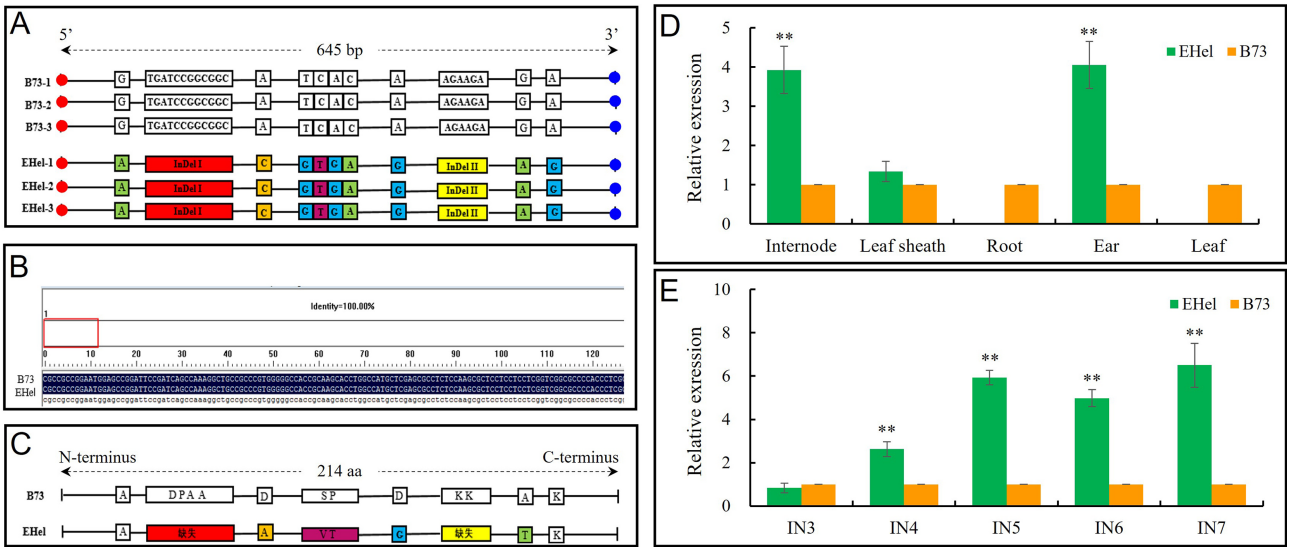

A: Sequence alignment of *Zm00001d016823* between B73 and EHel. Three independent sequences of *Zm00001d016823* were cloned from both B73 and EHel, and listed as −1/−2/−3, respectively. Red and blue dots correspondingly refer to the starting and ending codons. B: Sequence alignment of *Zm00001d016831* between B73 and EHel. C: Comparison of coding products by *Zm00001d016823* with the sequences from B73 and EHel, respectively. D and E: qRT-PCR assays of *Zm00001d016823* among different tissues (D) and different internodes (E) between B73 and EHel. ** in E and F refer to the significance level of $P < 0.01$ through *T*-test.

Figure 5. Chromosomal distribution of detected QTL and candidate validation of qILaa5.

The resultsof qRT-PCR assay showed that *Zm00001d016823* highly expressed in the tissues of internode and ear of EHel, while nearly no expression signals were observed in both tissues of root and leaf of EHel (Figure 5(D)). Considering the relative expression of *Zm00001d016823* among different internodes from IN3 to IN7 between EHel and B73, statistical higher expression levels were observed among the IN4 to IN7 of EHel than those of B73 (Figure 5(E)). The rela-

tive expression levels of *Zm00001d016823* among IN3 to IN7 exhibited negative correlation to the relative length of IN3 to IN7 ($R = -0.4165$, $P = 0.4854$), suggesting that *Zm00001d016823* might negatively regulate the internode length above the ear in maize.

4. Discussion

Moderate height is essential for the construction of idea plant type. In 1960s, numerous varieties with dwarf or semi-dwarf plant height, improved resistance, higher-yielding and better-quality performance were released in both rice and wheat, leading a revolution in the increasing of grains around the world, trigging a global Green Revolution [33]-[35]. Differed from both rice and wheat, maize possesses tall plant with higher PH, and corresponding higher EH. This special plant structure results in an inherent weakness of lodging, i.e., stalk lodging and root lodging, over strong winds [36]. It was documented that a record-breaking windstorm in 2020 swap across Iowa, destroyed about 16% maize production there, causing total losses of more than $10 billion [36]. Similar losses were also documented in other maize producing areas around the world [37]-[39]. Breeding novel maize varieties with shorter PH and EH might be the potential way out for lodging related resistances [40]. While few genes were discovered beyond phytohormone related pathways involving in regulating the development of internode no. and length, and then PH and EH, in maize.

In the present study, we identified 13 QTL for internode no. and length related traits in maize, including three major QTL for both internode no. and average internode length above ear (ILaa) (**Table 2**). Among all the annotated genes, *Zm00001d016823* was determined as the candidate of *qILaa*5, the major QTL for average internode length above ear in maize (**Table 2**, **Figure 5(A)**, **Figure 5(D)-(E)**). *Zm00001d016823* is annotated to encode a WEB family protein with unknown function (**Table 3**). WEB (Weak Chloroplast Movement under Blue Light) is a plant-specific protein with coiled-coil domain, and is reported to respond the chloroplast photo-relocation under different light intensities [41] [42]. The chloroplasts in the corresponding mutants of *web*1 and *web*2/*pmi*2 (*plastid movement impaired*2) in *Arabidopsis* are defective in moving toward or away from weak or strong light, respectively [41] [43]. Meanwhile, WEB1 can physically interact with WEB2/PMI2, forming a WEB1-PMI2 complex to suppress JAC1, another key protein with J-domain that essential for chloroplast moving toward weak light intensity [41] [42]. Except *Arabidopsis*, there are few documents focused on WEB gene family in other plants, especially WEB family members involved in controlling the phenotypic performance of internode length in maize.

We compared the relative expressions ratio of this gene between EHel to B73 and the corresponding relative internode length among INa4 to INa7 between EHel to B73. The results indicated a negative trend between the relative expression levels and the relative internode length, suggesting a negative regulating of *Zm00001d016823* to the average internode length above ears in maize. Considering

the annotated information, further functional dissection of *Zm00001d016823* might discovery novel molecular mechanism beyond phytohormone of WEB family member in controlling internode length and PH in maize, and will shed new light into the construction of ideotype with short stature for maize varieties.

5. Conclusion

In the present study, 13 QTL controlling four internode no. and length related traits in maize were identified, distributing on six chromosomes of Chr1, Chr2, and Chr5-8. Genomic annotation of *qILaa*5, the major QTL for average internode length above ear with the largest PVE suggests *Zm00001d016823* as the candidate. *Zm00001d016823* is annotated to encode the product that belongs to WEB protein family. Combined comparisons between the qRT-PCR assay and relative internode lengths of IN3 to IN7 showed negative correlation between the gene expression levels and the lengths of internodes above ear, implying a negative regulating of *Zm00001d016823* to the average internode length above ear in maize.

Funding

This work was supported by the project of Natural Science Foundation of Chongqing (2023NSCQ-MSX1359, cstc2021jcyj-msxmX0583), and the cooperation project of Exploration and Utilization of Maize Germplasm with Stress-Resistance, High Yield, and Better Quality in Southwestern Mountainous Areas.

Conflicts of Interest

The authors declare no conflicts of interest regarding the publication of this paper.

References

[1] Zhou, Z., Zhang, C., Lu, X., Wang, L., Hao, Z., Li, M., *et al*. (2018) Dissecting the Genetic Basis Underlying Combining Ability of Plant Height Related Traits in Maize. *Frontiers in Plant Science*, **9**, Article No. 1117. https://doi.org/10.3389/fpls.2018.01117

[2] Zhao, Y., Zhang, S., Lv, Y., Ning, F., Cao, Y., Liao, S., *et al*. (2022) Optimizing Ear-Plant Height Ratio to Improve Kernel Number and Lodging Resistance in Maize (*Zea mays* L.). *Field Crops Research*, **276**, Article ID: 108376. https://doi.org/10.1016/j.fcr.2021.108376

[3] Stubbs, C.J., Kunduru, B., Bokros, N., Verges, V., Porter, J., Cook, D.D., *et al*. (2023) Moving toward Short Stature Maize: The Effect of Plant Height on Maize Stalk Lodging Resistance. *Field Crops Research*, **300**, Article ID: 109008. https://doi.org/10.1016/j.fcr.2023.109008

[4] Wang, W., Guo, W., Le, L., Yu, J., Wu, Y., Li, D., *et al*. (2023) Integration of High-Throughput Phenotyping, GWAS, and Predictive Models Reveals the Genetic Architecture of Plant Height in Maize. *Molecular Plant*, **16**, 354-373. https://doi.org/10.1016/j.molp.2022.11.016

[5] Peiffer, J.A., Romay, M.C., Gore, M.A., Flint-Garcia, S.A., Zhang, Z., Millard, M.J.,

et al. (2014) The Genetic Architecture of Maize Height. *Genetics*, **196**, 1337-1356. https://doi.org/10.1534/genetics.113.159152

[6] Paciorek, T., Chiapelli, B.J., Wang, J.Y., Paciorek, M., Yang, H., Sant, A., *et al.* (2022) Targeted Suppression of Gibberellin Biosynthetic Genes *ZmGA20ox3* and *ZmGA20ox5* Produces a Short Stature Maize Ideotype. *Plant Biotechnology Journal*, **20**, 1140-1153. https://doi.org/10.1111/pbi.13797

[7] Fan, Y. and Li, Y. (2019) Molecular, Cellular and Yin-Yang Regulation of Grain Size and Number in Rice. *Molecular Breeding*, **39**, Article No. 163. https://doi.org/10.1007/s11032-019-1078-0

[8] Yuan, Z., Persson, S. and Zhang, D. (2020) Molecular and Genetic Pathways for Optimizing Spikelet Development and Grain Yield. *aBIOTECH*, **1**, 276-292. https://doi.org/10.1007/s42994-020-00026-x

[9] Mukherjee, A., Gaurav, A.K., Singh, S., Yadav, S., Bhowmick, S., Abeysinghe, S., *et al.* (2022) The Bioactive Potential of Phytohormones: A Review. *Biotechnology Reports*, **35**, e00748. https://doi.org/10.1016/j.btre.2022.e00748

[10] Dong, Z., Xiao, Y., Govindarajulu, R., Feil, R., Siddoway, M.L., Nielsen, T., *et al.* (2019) The Regulatory Landscape of a Core Maize Domestication Module Controlling Bud Dormancy and Growth Repression. *Nature Communications*, **10**, Article No. 3810. https://doi.org/10.1038/s41467-019-11774-w

[11] Castorina, G. and Consonni, G. (2020) The Role of Brassinosteroids in Controlling Plant Height in Poaceae: A Genetic Perspective. *International Journal of Molecular Sciences*, **21**, Article No. 1191. https://doi.org/10.3390/ijms21041191

[12] Cowling, C.L., Dash, L. and Kelley, D.R. (2023) Roles of Auxin Pathways in Maize Biology. *Journal of Experimental Botany*, **74**, 6989-6999. https://doi.org/10.1093/jxb/erad297

[13] Li, Q., Liu, N. and Wu, C. (2023) Novel Insights into Maize (*Zea mays*) Development and Organogenesis for Agricultural Optimization. *Planta*, **257**, Article No. 94. https://doi.org/10.1007/s00425-023-04126-y

[14] Cassani, E., Bertolini, E., Cerino Badone, F., Landoni, M., Gavina, D., Sirizzotti, A., *et al.* (2009) Characterization of the First Dominant Dwarf Maize Mutant Carrying a Single Amino Acid Insertion in the VHYNP Domain of the *Dwarf8* Gene. *Molecular Breeding*, **24**, 375-385. https://doi.org/10.1007/s11032-009-9298-3

[15] Chen, Y., Hou, M., Liu, L., Wu, S., Shen, Y., Ishiyama, K., *et al.* (2014) The Maize *DWARF1* encodes a Gibberellin 3-Oxidase and Is Dual Localized to the Nucleus and Cytosol. *Plant Physiology*, **166**, 2028-2039. https://doi.org/10.1104/pp.114.247486

[16] Lawit, S.J., Wych, H.M., Xu, D., Kundu, S. and Tomes, D.T. (2010) Maize DELLA Proteins Dwarf Plant8 and Dwarf Plant9 as Modulators of Plant Development. *Plant and Cell Physiology*, **51**, 1854-1868. https://doi.org/10.1093/pcp/pcq153

[17] Winkler, R.G. and Helentjaris, T. (1995) The Maize *Dwarf3* Gene Encodes a Cytochrome P450-Mediated Early Step in Gibberellin Biosynthesis. *The Plant Cell*, **7**, 1307-1317. https://doi.org/10.1105/tpc.7.8.1307

[18] Li, S., Sun, Z., Sang, Q., Qin, C., Kong, L., Huang, X., *et al.* (2023) Soybean *Reduced Internode 1* Determines Internode Length and Improves Grain Yield at Dense Planting. *Nature Communications*, **14**, Article No. 7939. https://doi.org/10.1038/s41467-023-42991-z

[19] Sun, C., Liu, Y., Li, G., Chen, Y., Li, M., Yang, R., *et al.* (2024) *ZmCYP90D1* Regulates Maize Internode Development by Modulating Brassinosteroid-Mediated Cell

Division and Growth. *The Crop Journal*, **12**, 58-67. https://doi.org/10.1016/j.cj.2023.11.002

[20] Wang, X., Ren, Z., Xie, S., Li, Z., Zhou, Y. and Duan, L. (2024) Jasmonate Mimic Modulates Cell Elongation by Regulating Antagonistic bHLH Transcription Factors via Brassinosteroid Signaling. *Plant Physiology*, kiae217. https://doi.org/10.1093/plphys/kiae217

[21] Le, L., Guo, W., Du, D., Zhang, X., Wang, W., Yu, J., *et al*. (2022) A Spatiotemporal Transcriptomic Network Dynamically Modulates Stalk Development in Maize. *Plant Biotechnology Journal*, **20**, 2313-2331. https://doi.org/10.1111/pbi.13909

[22] Wu, L., Zheng, Y., Jiao, F., Wang, M., Zhang, J., Zhang, Z., *et al*. (2022) Identification of Quantitative Trait Loci for Related Traits of Stalk Lodging Resistance Using Genome-Wide Association Studies in Maize (*Zea mays* L.). *BMC Genomic Data*, **23**, Article No. 76. https://doi.org/10.1186/s12863-022-01091-5

[23] Wang, X., Chen, Y., Sun, X., Li, J., Zhang, R., Jiao, Y., *et al*. (2022) Characteristics and Candidate Genes Associated with Excellent Stalk Strength in Maize (*Zea mays* L.). *Frontiers in Plant Science*, **13**, Article ID: 957566. https://doi.org/10.3389/fpls.2022.957566

[24] Gul, H., Qian, M., G. Arabzai, M., Huang, T., Ma, Q., Xing, F., *et al*. (2022) Discovering Candidate Chromosomal Regions Linked to Kernel Size-Related Traits via QTL Mapping and Bulked Sample Analysis in Maize. *Phyton*, **91**, 1429-1443. https://doi.org/10.32604/phyton.2022.019842

[25] Shi, Y.S., Li, Y., Wang, T.Y. and Song, Y.C. (2006) Description and Data Standard for Maize (*Zea mays* L.). China Agriculture Press. (In Chinese)

[26] Norman, P.E., Kamara, L., Beah, A., Gborie, K.S., Saquee, F.S., Kanu, S.A., *et al*. (2024) Genetic and Agronomic Parameter Estimates of Growth, Yield and Related Traits of Maize (*Zea mays* L.) under Different Rates of Nitrogen Fertilization. *American Journal of Plant Sciences*, **15**, 274-291. https://doi.org/10.4236/ajps.2024.154020

[27] Meng, L., Li, H., Zhang, L. and Wang, J. (2015) QTL Icimapping: Integrated Software for Genetic Linkage Map Construction and Quantitative Trait Locus Mapping in Biparental Populations. *The Crop Journal*, **3**, 269-283. https://doi.org/10.1016/j.cj.2015.01.001

[28] McCouch, S., Chao, Y.G., Yano, M., Paul, E., Blinstrub, M., Morishima, H. and Kinoshita, T. (1997) Report on QTL Nomenclature. *Rice Genetics Newsletter*, **14**, 111-131.

[29] Stuber, C.W., Lincoln, S.E., Wolff, D.W., Helentjaris, T. and Lander, E.S. (1992) Identification of Genetic Factors Contributing to Heterosis in a Hybrid from Two Elite Maize Inbred Lines Using Molecular Markers. *Genetics*, **132**, 823-839. https://doi.org/10.1093/genetics/132.3.823

[30] Walley, J.W., Sartor, R.C., Shen, Z., Schmitz, R.J., Wu, K.J., Urich, M.A., *et al*. (2016) Integration of Omic Networks in a Developmental Atlas of Maize. *Science*, **353**, 814-818. https://doi.org/10.1126/science.aag1125

[31] Xiao, Q., Huang, T., Zhou, C., Chen, W., Cha, J., Wei, X., *et al*. (2023) Characterization of Subunits Encoded by *SnRK1* and Dissection of Combinations among These Subunits in Sorghum (*Sorghum bicolor* L.). *Journal of Integrative Agriculture*, **22**, 642-649. https://doi.org/10.1016/j.jia.2022.08.068

[32] Livak, K.J. and Schmittgen, T.D. (2001) Analysis of Relative Gene Expression Data Using Real-Time Quantitative PCR and the $2^{-\Delta\Delta CT}$ Method. *Methods*, **25**, 402-408. https://doi.org/10.1006/meth.2001.1262

[33] Khush, G.S. (2001) Green Revolution: The Way Forward. *Nature Reviews Genetics*, **2**, 815-822. https://doi.org/10.1038/35093585

[34] Briggs, J. (2009) Green Revolution. In: Kitchin, R. and Thrift, N., Eds., *International Encyclopedia of Human Geography*, Elsevier, 634-638.

[35] Pingali, P.L. (2012) Green Revolution: Impacts, Limits, and the Path Ahead. *Proceedings of the National Academy of Sciences*, **109**, 12302-12308. https://doi.org/10.1073/pnas.0912953109

[36] Stokstad, E. (2023) High Hopes for Short Corn. *Science*, **382**, 364-367. https://doi.org/10.1126/science.adl5302

[37] Shah, A.N., Tanveer, M., Rehman, A.u., Anjum, S.A., Iqbal, J. and Ahmad, R. (2016) Lodging Stress in Cereal—Effects and Management: An Overview. *Environmental Science and Pollution Research*, **24**, 5222-5237. https://doi.org/10.1007/s11356-016-8237-1

[38] Xue, J., Xie, R., Zhang, W., Wang, K., Hou, P., Ming, B., *et al*. (2017) Research Progress on Reduced Lodging of High-Yield and -Density Maize. *Journal of Integrative Agriculture*, **16**, 2717-2725. https://doi.org/10.1016/s2095-3119(17)61785-4

[39] Zhang, P., Gu, S., Wang, Y., Xu, C., Zhao, Y., Liu, X., *et al*. (2023) The Relationships between Maize (*Zea mays* L.) Lodging Resistance and Yield Formation Depend on Dry Matter Allocation to Ear and Stem. *The Crop Journal*, **11**, 258-268. https://doi.org/10.1016/j.cj.2022.04.020

[40] Li, W., Ge, F., Qiang, Z., Zhu, L., Zhang, S., Chen, L., *et al*. (2019) Maize *ZmRPH1* Encodes a Microtubule-Associated Protein That Controls Plant and Ear Height. *Plant Biotechnology Journal*, **18**, 1345-1347. https://doi.org/10.1111/pbi.13292

[41] Kodama, Y., Suetsugu, N., Kong, S. and Wada, M. (2010) Two Interacting Coiled-Coil Proteins, WEB1 and PMI2, Maintain the Chloroplast Photorelocation Movement Velocity in *Arabidopsis*. *Proceedings of the National Academy of Sciences*, **107**, 19591-19596. https://doi.org/10.1073/pnas.1007836107

[42] Kodama, Y., Suetsugu, N. and Wada, M. (2011) Novel Protein-Protein Interaction Family Proteins Involved in Chloroplast Movement Response. *Plant Signaling & Behavior*, **6**, 483-490. https://doi.org/10.4161/psb.6.4.14784

[43] Luesse, D.R., DeBlasio, S.L. and Hangarter, R.P. (2006) *Plastid Movement Impaired 2*, a New Gene Involved in Normal Blue-Light-Induced Chloroplast Movements in *Arabidopsis*. *Plant Physiology*, **141**, 1328-1337. https://doi.org/10.1104/pp.106.080333